

Forced convection boundary layer flow and heat transfer along a flat plate embedded in a porous medium

C. BECKERMANN and R. VISKANTA

Heat Transfer Laboratory, School of Mechanical Engineering, Purdue University,
 West Lafayette, IN 47907, U.S.A.

(Received 15 July 1986 and in final form 5 December 1986)

1. INTRODUCTION

DURING the past decade, fluid flow and heat transfer through porous media have experienced renewed research interest due to a broad range of applications, including geothermal systems, thermal insulation, metals processing, catalytic reactors, direct-contact heat exchangers, transpiration cooling, filtration, etc. In many practical systems, the porous medium has a high permeability (i.e. the porous media Reynolds numbers are high) and is bounded by an impermeable wall, making Darcy's law inapplicable. This has led to the inclusion of inertia and boundary effects in recent studies of fluid flow through porous media. Inertia effects can be included in the momentum equation through the so-called Forchheimer's extension [1], where Darcy's law is modified by the addition of a quadratic term in velocity. The boundary effects can be modeled through the inclusion of a viscous shear stress term, which has become known as Brinkman's extension [2].

Inertia, boundary and variable-porosity effects have been studied extensively [3-6] in forced convection boundary layer flow and heat and mass transfer along a flat plate embedded in a porous medium. Vafai and Tien [4] have solved the governing equations numerically and found that the velocity boundary layer develops in a short distance from the leading edge, while its thickness is of the order $\sqrt{(K/\epsilon)}$. On the other hand, the boundary effects can significantly alter the heat transfer from the plate, especially at high Prandtl numbers. As expected, the inertia effects are more pronounced in high permeability porous media and in low viscosity fluids.

In the present study, the problem of forced convection flow and heat transfer along a flat plate in a porous medium is reexamined by including both, the inertia and boundary effects, while porosity variations close to the wall are not considered. Since the developing part of the momentum boundary layer has been found to be negligibly small [4], it is not included in the present analysis. For the case of the fully-developed momentum boundary layer, closed-form expressions are derived for the velocity and temperature profiles. From these results, the wall shear stress and the Nusselt number are determined as functions of modified Reynolds and Prandtl numbers. In addition, comparisons are made with the limiting cases of no inertia and/or boundary effects. Finally, several results are presented for the case of blowing in the wall bounding the porous medium.

2. GOVERNING EQUATIONS

A schematic of the physical model and coordinate system is shown in Fig. 1. In the present analysis, the flow is assumed to be steady, incompressible, and two-dimensional. The thermophysical properties of the fluid are assumed to be constant. The porous medium is considered homogeneous and isotropic and is saturated with a fluid which is in local thermodynamic equilibrium with the solid matrix. Employing the usual boundary layer approximations, the governing equations can be written in terms of the superficial (Darcian) velocity as [7]:

continuity

$$\frac{\partial U_D}{\partial X} + \frac{\partial V_D}{\partial Y} = 0; \tag{1}$$

momentum

$$0 = -\frac{\partial P}{\partial X} + \mu_{\text{eff}} \frac{\partial^2 U_D}{\partial Y^2} - \left(\frac{\mu_f}{K} + \frac{\rho C}{\sqrt{K}} |U_{\text{bl}}| \right) U_D; \tag{2}$$

$$0 = -\frac{\partial P}{\partial Y}; \tag{3}$$

energy

$$U_D \frac{\partial T}{\partial X} + V_D \frac{\partial T}{\partial Y} = \alpha_{\text{eff}} \frac{\partial^2 T}{\partial Y^2} \tag{4}$$

where

$$|U_{\text{bl}}| = \sqrt{(U_D^2 + V_D^2)}.$$

It should be noted that, due to the inclusion of Forchheimer's extension in the momentum equation (2), the above set of equations is valid for laminar, transition and turbulent flow [8]. At low velocities, Forchheimer's extension becomes insignificant and Darcy's law is recovered. In the transition and turbulent regime, inertia effects (i.e. separation and wake effects) become important, which are proportional to the square of the velocity [9]. The value of the inertia coefficient C in Forchheimer's extension has been measured experimentally by Ward [8]. Although it is now generally accepted that C is a function of the microstructure of the porous medium [10, 11], Ward has found that for a large variety of porous media, C can be taken as a constant equal to approximately 0.55.

There has been some controversy about the value of μ_{eff} in Brinkman's extension in equation (2) [12]. As a first approximation, μ_{eff} is being taken equal to μ_f in the present study. The effective thermal diffusivity, α_{eff} , in equation (3) accounts for differences in the thermal conductivities of the fluid and the solid, as well as for thermal dispersion effects.

With the foregoing simplification, the governing equations can be cast into dimensionless form (see the nomenclature section for the definitions of the dimensionless variables). Omitting the y -momentum equation (3), the dimensionless

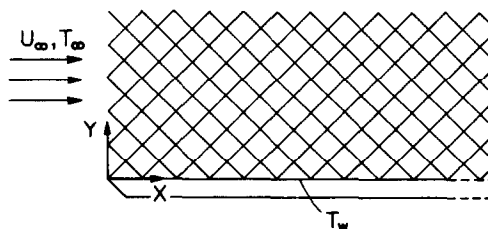


FIG. 1. Schematic of the physical model and coordinate system.

NOMENCLATURE

| | |
|-------|--|
| c | constant close to unity |
| c_p | specific heat [$\text{J kg}^{-1} \text{K}^{-1}$] |
| C | inertia coefficient |
| h | convective heat transfer coefficient [$\text{W m}^{-2} \text{K}^{-1}$] |
| k | thermal conductivity [$\text{W m}^{-1} \text{K}^{-1}$] |
| K | permeability of the porous medium [m^2] |
| Nu | Nusselt number, defined by equation (12) |
| P | pressure [N m^{-2}] |
| Pr | modified Prandtl number, defined by equation (10) |
| Re | modified Reynolds number, defined by equation (9) |
| T | temperature [K] |
| u | dimensionless x -component velocity, U_D/U_c |
| U_D | x -component of the Darcian velocity [m s^{-1}] |
| U_c | characteristic velocity, $-(dP/dX)K/\mu_f$ |
| v | dimensionless y -component velocities, V_D/U_c |
| v_w | dimensionless blowing velocity at the wall, V_w/U_c |
| V_D | y -component of the Darcian velocity [m s^{-1}] |
| x | dimensionless horizontal coordinate, X/\sqrt{K} |
| X | horizontal coordinate [m] |
| y | dimensionless vertical coordinate, Y/\sqrt{K} |
| Y | vertical coordinate [m] |
| z | local variable, defined by equation (21). |

Greek symbols

| | |
|-----------------------|---|
| α_{eff} | effective thermal diffusivity, $k_{\text{eff}}/\rho c_{p,f}$ [$\text{m}^2 \text{s}^{-1}$] |
| Γ | complete gamma function |
| δ_c | dimensionless momentum boundary layer thickness, Δ_c/\sqrt{K} |
| δ_T | dimensionless thermal boundary layer thickness, Δ_T/\sqrt{K} |
| Δ | boundary layer thickness [m] |
| ε | porosity of the porous medium |
| Θ | dimensionless temperature, $(T - T_w)/(T_\infty - T_w)$ |
| μ | dynamic viscosity [N s m^{-2}] |
| ν | kinematic viscosity [$\text{m}^2 \text{s}^{-1}$] |
| ξ | similarity variable, defined by equation (31) |
| ρ | fluid density [kg m^{-3}] |
| τ_w | dimensionless wall shear stress, defined by equation (11). |

Subscripts

| | |
|----------|--|
| D | Darcy |
| eff | effective |
| f | fluid |
| f.d. | fully developed |
| w | wall |
| 3 | third root, see equation (19) |
| ∞ | at infinity, i.e. outside of the boundary layer. |

equations are:

continuity

$$\frac{\partial u}{\partial x} + \frac{\partial v}{\partial y} = 0; \quad (5)$$

momentum

$$0 = 1 + \frac{\partial^2 u}{\partial y^2} - u - Re|u|u; \quad (6)$$

energy

$$u \frac{\partial \Theta}{\partial x} + v \frac{\partial \Theta}{\partial y} = \frac{1}{Re Pr} \frac{\partial^2 \Theta}{\partial y^2}. \quad (7)$$

The boundary conditions are given by:

$$\begin{aligned} \text{at } x = 0: \quad & u = u_x, \quad \Theta = 1 \\ \text{at } y = 0: \quad & u = 0, \quad v = v_w, \quad \Theta = 0 \\ \text{at } y \rightarrow \infty \quad & u = u_\infty, \quad \frac{\partial u}{\partial y} = \frac{\partial^2 u}{\partial y^2} = 0, \\ & \Theta = 1, \quad \frac{\partial \Theta}{\partial y} = 0. \end{aligned} \quad (8)$$

From equation (6) we can see that the momentum boundary layer is governed by a single parameter which is the product of the conventional porous media Reynolds number and the inertia coefficient. This modified Reynolds number is defined as

$$Re = \frac{U_c \sqrt{KC}}{\nu}. \quad (9)$$

The Reynolds number appears directly due to the inclusion of the inertia term. Thus, omitting the inertia term is equivalent to assuming that the Reynolds number is equal to zero.

The thermal boundary layer is governed by the product of the modified Reynolds and Prandtl numbers, where the modified Prandtl number is defined as

$$Pr = \frac{\nu}{\alpha_{\text{eff}} C}. \quad (10)$$

A similar definition of the modified Prandtl number has also been found useful by Jonsson and Catton [13] in correlating natural convection data. Interestingly, the ratio ν/C appears in both, the Reynolds and Prandtl numbers. Therefore, an effective viscosity could be defined as $\nu_{\text{eff}} \equiv \nu/C$, which is, similar to the effective thermal diffusivity α_{eff} , dependent on the properties of the porous medium and the fluid.

The results for the shear stress and the heat transfer rate at the impermeable wall are presented in terms of the dimensionless wall shear stress and the Nusselt number, defined as

$$\tau_w = \left. \frac{\partial u}{\partial y} \right|_{y=0} \quad (11)$$

$$Nu = \frac{h\sqrt{K}}{k_{\text{eff}}} = \left. \frac{\partial \Theta}{\partial y} \right|_{y=0}. \quad (12)$$

3. SOLUTIONS FOR THE FULLY-DEVELOPED MOMENTUM BOUNDARY LAYER

As pointed out by Vafai and Tien [4] the fully developed momentum boundary layer is a unique feature of flow in porous media. In the fully-developed region, we have that $\partial u/\partial x = 0$ and, hence, it follows from the continuity equation that $v = 0$ (for the case of no blowing at the wall). Therefore, the governing equations reduce to

$$\frac{d^2 u}{dy^2} = u + Re u^2 - 1 \quad (13)$$

$$u(y) \frac{\partial \Theta}{\partial x} = \frac{1}{Re Pr} \frac{\partial^2 \Theta}{\partial y^2}. \quad (14)$$

Since $d^2 u/dy^2 = 0$ at $y \rightarrow \infty$, we obtain from equation (13) that

$$u_\infty = \frac{\sqrt{(1+4Re)} - 1}{2Re}. \quad (15)$$

3.1. Momentum boundary layer

A closed-form analytical solution of equation (13), together with the boundary conditions, equation (8), can be obtained by multiplying equation (13) by $2 du/dy$ and then integrating from y to ∞ . The resulting equation is

$$\frac{\partial u}{\partial y} = \left[u^2 - u_\infty^2 + \frac{2}{3} Re(u^3 - u_\infty^3) - 2(u - u_\infty) \right]^{1/2}. \quad (16)$$

Hence, the wall shear stress for the fully-developed velocity field is found to be

$$\tau_w = \left[2u_x - u_\infty^2 - \frac{2}{3} Re u_x^3 \right]^{1/2} \quad (17)$$

where u_∞ is given by equation (15). Note that for $Re \rightarrow 0$ (i.e. no inertia term), both u_∞ and τ_w approach unity. Separating variables and integrating from 0 to y , equation (16) can be written as

$$\int_0^y \frac{du^*}{(u_\infty - u^*)\sqrt{(u^* - u_3)}} = \frac{\sqrt{(2Re)}}{3} y \quad (18)$$

where

$$u_3 = u_\infty + \frac{3}{2Re} - \frac{3}{Re u_\infty} < 0 \quad (19)$$

is the third real root of the right-hand side of equation (16). Performing the integration, the fully-developed velocity profile is found to be

$$u = u_3 + (u_\infty - u_3) \left[\frac{z+1}{z-1} \right]^2 \quad (20)$$

where

$$z = \frac{[\sqrt{-u_3} + \sqrt{(u_\infty - u_3)}] \exp[\sqrt{(2/3)(u_\infty - 1)}y]}{[\sqrt{-u_3} - \sqrt{(u_\infty - u_3)}]} \quad (21)$$

The velocity profile expressed by equation (20) approaches asymptotically a simple exponential profile as $Re \rightarrow 0$, given by the solution of equation (13) for $Re = 0$, i.e.

$$u = 1 - e^{-y}. \quad (22)$$

Due to the exponential nature of the velocity profile, it is difficult to define a meaningful velocity boundary layer thickness. If we define the boundary layer thickness as the point where u becomes cu_∞ , where c is some constant close to unity, we obtain to a good approximation

$$\delta_c \approx \ln \left[\frac{1}{1-c} \right] \left[\frac{2}{u_r} - 1 \right]^{-0.5} \quad (23)$$

or

$$\delta_c \approx \ln \left[\frac{1}{1-c} \right] \left[\frac{4Re}{\sqrt{(1+4Re)} - 1} - 1 \right]^{-0.5}. \quad (24)$$

3.2. Thermal boundary layer

Unlike the momentum boundary layer, the thermal boundary layer does not reach a fully-developed condition. In the solution of the energy equation, equation (14), it is assumed that the impermeable wall is insulated up to the point where the momentum boundary layer is fully developed. Due to the complicated nature of the velocity profile, equation (20), a closed-form solution of equation (14) does not appear possible. However, two approximate solutions can be obtained by considering the cases of very small and very large Prandtl numbers. In the first case the thermal boundary layer thickness is much larger than the velocity boundary layer thickness and the velocity profile can be approximated by

$$u(y) = u_\infty \quad (Pr \rightarrow 0). \quad (25)$$

Together with the boundary conditions, equation (8), the solution of equation (14) is now easily obtained as

$$\Theta = \operatorname{erf} \left[\sqrt{(Re Pr u_\infty/x)} \frac{y}{2} \right]. \quad (Pr \rightarrow 0). \quad (26)$$

The thermal boundary layer thickness and the Nusselt number are given by

$$\delta_T \approx 6.0 \sqrt{\left(\frac{x}{Re Pr u_\infty} \right)} \quad (Pr \rightarrow 0) \quad (27)$$

$$Nu = (\pi x)^{-1/2} (Re Pr u_\infty)^{1/2} \quad (Pr \rightarrow 0) \quad (28)$$

or by substituting equation (15), equation (28) becomes

$$Nu = (2\pi x)^{-1/2} Pr^{1/2} (\sqrt{(1+4Re)} - 1)^{1/2} \quad (Pr \rightarrow 0). \quad (29)$$

For very large Reynolds numbers, the Nusselt number varies approximately as $Nu \propto Re^{1/4}$. For very small Reynolds numbers, i.e. $Re \rightarrow 0$ (i.e. negligible inertia effects) u_∞ approaches unity and the Nusselt number is proportional to $Re^{1/2}$. In addition, the above solution with $u_\infty = 1$ is also the exact solution for the case of no inertia and boundary effects (but any Prandtl number). Hence, if both, the Reynolds and Prandtl numbers are small, Darcy's law (i.e. $u = 1$) can safely be used in calculating the heat transfer rate from the impermeable wall.

In the asymptotic limit of very large Prandtl numbers, the thermal boundary layer is completely confined inside the momentum boundary layer. Leveque [14] has proposed that for this case, the velocity distribution inside the thermal boundary layer can be approximated by

$$u = \tau_w y \quad (Pr \rightarrow \infty). \quad (30)$$

Introducing the similarity variable

$$\xi = y \left(\frac{Re Pr \tau_w}{9x} \right)^{1/3} \quad (31)$$

the energy equation is transformed into the following ordinary differential equation

$$\frac{d^2 \Theta}{d\xi^2} + 3\xi^2 \frac{d\Theta}{d\xi} = 0. \quad (32)$$

With the boundary conditions

$$\Theta(0) = 0 \quad \text{and} \quad \Theta(\infty) = 1 \quad (33)$$

the solution of equation (32) is given by

$$\Theta = \frac{d\Theta}{d\xi} \Big|_{\xi=0} \int_0^{\xi} \exp(-\zeta^3) d\zeta \quad (Pr \rightarrow \infty) \quad (34)$$

where

$$\frac{d\Theta}{d\xi} \Big|_{\xi=0} = \frac{1}{\Gamma(4/3)} = 1.12. \quad (35)$$

From the above solution, we can obtain the following Nusselt number relation

$$Nu = 0.5384 \left(\frac{Re Pr \tau_w}{x} \right)^{1/3} \quad (Pr \rightarrow \infty) \quad (36)$$

where τ_w is given by equation (17) as a function of the Reynolds number. Again, for very large Reynolds numbers the Nusselt number is approximately proportional to $Re^{1/4}$, while for $Re \rightarrow 0$ (i.e. negligible inertia effects) τ_w approaches unity and $Nu \propto Re^{1/3}$.

The range of validity of the Nusselt number expressions for the two limiting cases $Pr \rightarrow 0$ and $Pr \rightarrow \infty$ (i.e. equation (29) and equation (36), respectively) will be further discussed in Section 5.

4. SOLUTION FOR THE FULLY-DEVELOPED BOUNDARY LAYER WITH BLOWING

In this section, some preliminary results are presented for the case where there is blowing at the wall bounding the porous medium, i.e. $v|_{y=0} = v_w$. From the continuity equation (5), we have for the fully-developed case

$$\frac{\partial v}{\partial y} = 0 \quad (37)$$

and hence

$$v(y) = v_w \quad (38)$$

Thus, the momentum and energy equations, equations (6) and (7), can now be written, respectively, as

$$0 = 1 + \frac{d^2 u}{dy^2} - u - Re u \sqrt{u^2 + v_w^2} \quad (39)$$

$$u \frac{\partial \Theta}{\partial x} + v_w \frac{\partial \Theta}{\partial y} = \frac{1}{Re Pr} \frac{\partial^2 \Theta}{\partial y^2} \quad (40)$$

and the boundary conditions are given by equation (8). Note that blowing does affect the fully-developed velocity profile through the inertia term in equation (39). The velocity at $y \rightarrow \infty$, i.e. u_x , is now given by the root of the equation

$$1 = u_x + Re u_x \sqrt{u_x^2 + v_w^2} \quad (41)$$

Following a similar procedure as in Section 3, we obtain for the wall shear stress the result

$$\tau_w = \left[\frac{2}{3} Re v_w^3 + 2u_x - u_x^2 - \frac{2}{3} Re(u_x^2 + v_w^2)^{3/2} \right]^{1/2} \quad (42)$$

where u_x is given by equation (41). The solution of equation (39) can be expressed as

$$\int_0^u \frac{du^*}{\left[(u^{*2} + v_w^2)^{3/2} - (u_x + v_w)^{3/2} + \frac{3}{2Re} (u^{*2} - u_x^2) - \frac{3}{Re} (u^* - u_x) \right]^{1/2}} = \sqrt{(2/(3Re))y} \quad (43)$$

The integral in the above equation is easily evaluated using standard numerical quadratures. The results for the velocity profile are presented in the following section.

Because of the complicated nature of the velocity profile in the case of blowing, no further attempt has been made to solve the energy equation (40). For the limiting cases of $Pr \rightarrow 0$ and $Pr \rightarrow \infty$ (refer to Section 3), similarity solutions to the energy equation can only be obtained if $v_w \sim x^{-1/2}$ for $Pr \rightarrow 0$, and $v_w \sim x^{-1/3}$ for $Pr \rightarrow \infty$. Estimates for the Nusselt number for the asymptotic cases $Pr \rightarrow 0$ and $Pr \rightarrow \infty$ can, however, be made by using equations (41) and (42) for u_x and τ_w , respectively, in the expressions for the Nusselt number derived in Section 3 for no blowing [equation (28) for $Pr \rightarrow 0$ and equation (36) for $Pr \rightarrow \infty$]. This procedure is equivalent to neglecting the term $v_w(\partial\Theta/\partial y)$ in the energy equation (40). A perturbation analysis shows that these estimates are accurate to $O(v_w)$ and, hence, they will only be reasonable for small blowing velocities.

5. RESULTS AND DISCUSSION

The results for the fully-developed momentum boundary layer are shown in Figs. 2-4. A comparison of the velocity profiles for the cases with and without blowing is given in Fig. 2. It can be seen that with increasing Reynolds number both the velocity at the edge of the boundary layer (u_x) and the boundary layer thickness (δ_c) decrease. This can be explained by the fact that with increasing Reynolds number the dimensionless velocities in the porous medium decrease due to the increase in the inertial drag. In reality, Reynolds numbers greater than about 1000 would be difficult to achieve. As expected, with blowing at the wall, the boundary layer thickness is slightly larger, while the u -velocities are

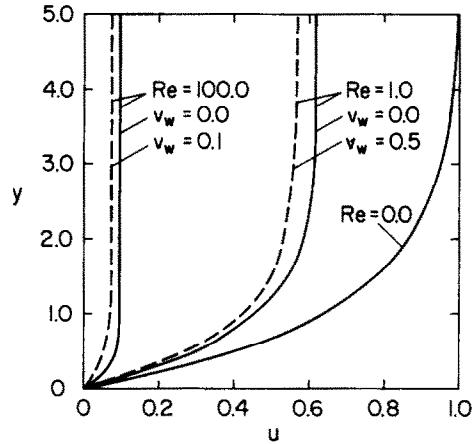


FIG. 2. Fully-developed velocity profiles (with and without blowing).

smaller when compared to the case of no blowing and the same Reynolds number. Additional calculations have shown that a good approximation to the velocity profile [equation (20)] can be obtained for all Reynolds numbers (less than about 100) by the equation

$$\frac{u}{u_x} = 1 - (1 - c)^{(y/\delta_c)} \quad (44)$$

where u_x and δ_c are calculated from equations (15) and (24), respectively, and, as before, c is a constant close to unity.

The dependence of the wall shear stress on the Reynolds

number and blowing at the wall, as given by equations (17) and (42), is illustrated in Fig. 3. It can be seen that the dimensionless wall shear stress approaches unity for $Re \rightarrow 0$ and zero for $Re \rightarrow \infty$. A high Reynolds number can be achieved by a high pressure drop, a high permeability or a low fluid viscosity. Actually, the dimensional wall shear stress decreases with increasing permeability and decreasing fluid viscosity, but increases for a higher pressure drop. In

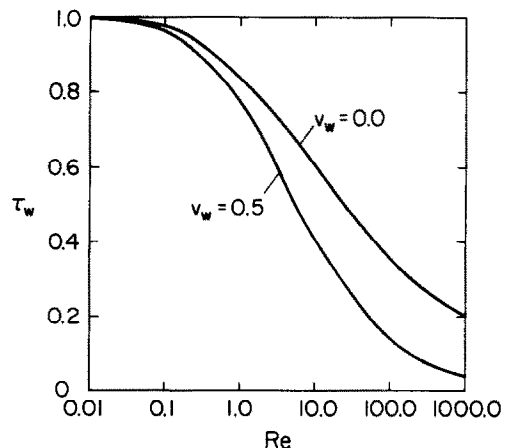


FIG. 3. Effect of Reynolds number on the wall shear stress for a fully-developed momentum boundary layer (with and without blowing).

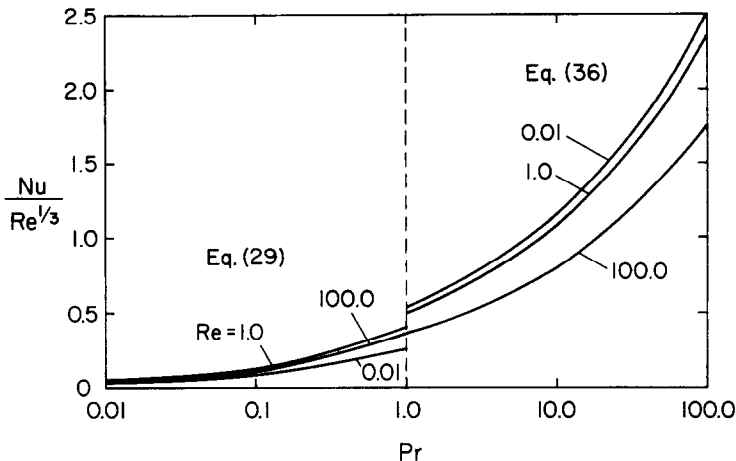


FIG. 4. Effect of Prandtl number on the Nusselt number for a fully-developed momentum boundary layer (at $x = 1.0$).

addition, Fig. 3 shows that, as expected, the wall shear stress is lower for the case of blowing at the wall.

The Nusselt number expressions derived in Section 3 for the limiting cases of $Pr \rightarrow 0$ [equation (29)] and $Pr \rightarrow \infty$ [equation (36)] are plotted as a function of the Prandtl number in Fig. 4. It can be seen that the differences in the Nusselt number calculated from the two equations are fairly small at Prandtl numbers of the order one. Hence, equation (29) can safely be used for Prandtl numbers up to about 0.5, while equation (36) can be used for Prandtl numbers greater than about 10.0. The Nusselt number can be appropriately interpolated from the two equations for intermediate values of the Prandtl number in a manner suggested by Churchill and Usagi [15]. The first-order estimate proposed in Section 4 for the Nusselt number in the case of blowing at the wall shows that, in this case, the Nusselt number will be smaller than in the case of no blowing, which is due to the decrease in u_∞ and τ_w [see equations (28) and (36)].

6. CONCLUSIONS

The problem of forced convection boundary layer flow and heat transfer along a flat plate embedded in a porous medium is studied by including both, inertia and boundary effects. It is found that the momentum and thermal boundary layers are governed by modified Reynolds and Prandtl numbers. For the case of a fully-developed momentum boundary layer, a closed-form analytical solution is derived for the velocity profile (with and without blowing), while approximate solutions are given for the temperature profile. It is shown that the velocity profile is basically of exponential nature, while the velocity boundary layer thickness decreases with increasing Reynolds number. In addition, simple expressions are given for the wall shear stress and the Nusselt number. In the case of blowing at the wall, the velocities, the wall shear stress, and the Nusselt number are smaller than in the case of no blowing and the same Reynolds and Prandtl numbers.

In conclusion, it can be said that neglecting the inertia and boundary effects can lead to serious errors for Reynolds numbers greater than 0.01. Utilizing similar mathematical procedures as presented in the previous sections, closed-form solutions can also be obtained, for example, for fully-developed porous media flow in a circular pipe or a parallel plate channel [16] and there is no need for omitting the nonlinear inertia term. It should be noted, however, that porosity variations near the wall, as present, for example, in packed beds of spheres, will alter the present analysis considerably due to channeling of the flow near the wall.

REFERENCES

1. P. Forchheimer, Wasserbewegung durch Boden, *Z. Ver. dt. Ing.* **45**, 1782–1788 (1901).
2. H. C. Brinkman, A calculation of the viscous force exerted by a flowing fluid on a dense swarm of particles, *Appl. Scient. Res.* **1**, 27–34 (1947).
3. K. Vafai and C. L. Tien, Boundary and inertia effects on convective mass transfer in porous media, *Int. J. Heat Mass Transfer* **25**, 1183–1190 (1980).
4. K. Vafai and C. L. Tien, Boundary and inertia effects on flow and heat transfer in porous media, *Int. J. Heat Mass Transfer* **24**, 195–203 (1981).
5. K. Vafai, Convective flow and heat transfer in variable-porosity media, *J. Fluid Mech.* **147**, 233–259 (1984).
6. K. Vafai, R. L. Alkire and C. L. Tien, An experimental investigation heat transfer in variable porosity media, *ASME J. Heat Transfer* **107**, 642–647 (1985).
7. C. L. Tien and J. T. Hong, Natural convection in porous media under non-Darcian and non-uniform permeabilities conditions. In *Natural Convection* (Edited by S. Kakac, W. Aung and R. Viskanta), pp. 573–587. Hemisphere, Washington, D.C. (1985).
8. J. C. Ward, Turbulent flow in porous media, *J. Hydraul. Div. ASCE* **90**, 1–12 (1964).
9. D. E. Wright, Nonlinear flow through granular media, *J. Hydraul. Div. ASCE* **94**, 851–872 (1968).
10. G. S. Beavers and E. M. Sparrow, Non-Darcy flow through fibrous porous media, *J. Appl. Mech.* **36**, 711–714 (1969).
11. S. Ergun, Fluid flow through packed columns, *Chem. Engng Prog.* **48**, 89–94 (1952).
12. S. Kim and W. B. Russel, Modelling of porous media by renormalization of the Stokes equations, *J. Fluid Mech.* **154**, 269–286 (1985).
13. T. Jonsson and I. Catton, Prandtl number dependence of natural convection in porous medium. In *Heat Transfer in Porous Media and Particulate Flows* (Edited by L. S. Yao, M. M. Chen, C. E. Hickox, P. G. Simpkins, L. C. Chow, M. Kaviany, P. Cheng and L. R. Davis), pp. 21–29. ASME, New York (1985).
14. M. A. Leveque, Les Lois de la Transmission de Chaleur par Convection, *Ann. Mines* **13**, 201–239 (1928).
15. S. W. Churchill and R. Usagi, A general expression for the correlation of rates of transfer and other phenomena, *A.I.Ch.E. J.* **18**, 1121–1128 (1972).
16. M. Kaviany, Laminar flow through a porous channel bounded by isothermal parallel plates, *Int. J. Heat Mass Transfer* **28**, 851–858 (1985).